POTENTIALS AND CHALLENGES OF SNOW DRIFT SIMULATION FOR AVALANCHE WARNING

Simon Schneiderbauer[1,2], **Peter Fischer[3]**, Arnulf Wurzer[4] and Arnold Studeregger[5]

ABSTRACT

The current understanding of snow drift modelling is reviewed. To overcome the most critical modelling issues of the state of the art models a continuum approach for advanced snow drift modelling is presented. This includes time dependent boundary conditions (BCs) from Numerical Weather Prediction (NWP) models, turbulent air flow and changing topography of the snow cover. This model is used to investigate snow transport at the Planneralm test site (Styria, Austria). Parameter studies show that the driving wind field is the most sensitive modelling parameter. Finally, the model is validated by two years of measurements from weather stations at the Planneralm (Austria, Styria), where two characteristic snow drift events are discussed in detail.

Keywords: snow drift, avalanche warning, CFD, optimization, time dependent boundary conditions, algebraic slip model, aerodynamic entrainment

INTRODUCTION

Snow avalanches are mostly triggered by a critical snow depth. The highest snow depths are generally accumulated in leeward slopes, chutes, and dingles, mainly caused by wind and snow drift. In addition freshly fallen snow contributes significantly to the total snow on mountainsides. Even on mountainsides with a slope angle as low as 30°, high snow depth significantly increases avalanche danger. Drifting snow also forms large snow cornices at mountain ridges. If those cornices break off they may trigger avalanches.

Up to now the evaluation of avalanche danger depends on the knowledge of the properties of the snow cover, the available meteorological data and the interpretation of meteorological data (Studeregger et al., 2012). Following this approach it is possible to identify regional levels of avalanche hazard (for a definition of what constitutes a hazard, see, e.g., Fell and others, 2005), but the outcome is often not satisfactory for avalanche warning services for assessing the avalanche danger on small scales.

The determination of snowdrift occurrences at critical local failure scars is limited by these common methods. Due to low visibility during snowstorms it is not possible to evaluate the different snow layers. In fact the avalanche professionals are aware of the existence of a critical snow layer, but it is very difficult to examine from the valley the amount of accumulated snow at potential avalanche fracture zones.

The numerical simulation of snowdrift supplies an area-wide distribution of the snow depth. A numerical approach should include time dependent geometries of the snow cover and complex particle transport phenomena. Additionally, the erosion and accumulation of snow particles leads to

[1] Dr. Simon Schneiderbauer. Christian Doppler Laboratory on Particulate Flow Modelling, Johannes Kepler University Linz, Austria

[2] DTECH Steyr, Austria

[3] Dr. Peter Fischer. DTECH Steyr, Steyrerweg 2, A-4400 Steyr, Austria (e-mail: peter.fischer@dtech-steyr.com)

[4] Mag. Arnulf Wurzer. Zentralanstalt für Meteorologie und Geodynamik, Austria

[5] Dr. Arnold Studeregger. Zentralanstalt für Meteorologie und Geodynamik, Austria

the creation of snow cornices and other wind-shaped formations. These deformations of the shape of the snow pack couple to the wind field and thus the flow is changed by the new geometry.

As an additional important issue the selection of appropriate boundary conditions for calculating the wind field has to be taken into account. In first place data from weather stations, which are located in the simulation area, can be used to determine the boundary conditions by applying an optimisation approach (Schneiderbauer and Pirker, 2010). If there is no station data available, the boundary conditions can be provided by local weather models (Schneiderbauer and Pirker, 2011).

In this work a short review of potentials and challenges for snow drift simulation models is given. An enhanced snow drift model will be presented including (a) a multiphase algebraic slip approach, (b) time dependent boundary conditions (BCs) from Numerical Weather Prediction (NWP) models and (c) turbulent air flow. Parameter studies evaluate the influence of snow properties in comparison to wind speed. Finally, the model is validated by measurements from weather stations at the Planneralm (Austria, Styria, see figure 1).

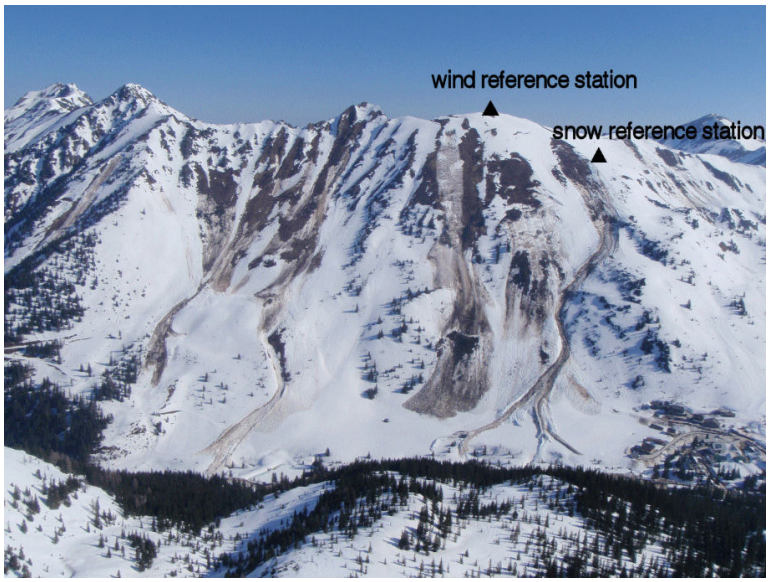

Fig. 1 Planneralm test site (source: Avalanche service Styria, Austria)

REVIEW OF SNOW DRIFT MODELS

The foundation for our current understanding of aeolian snow and sand transport was introduced by Bagnold (1941).

In the 90's, a more formalized classification of wind induced particle transport and a deeper understanding of the saltation transport mode was achieved (Pomeroy and Gray, 1990; Anderson and Haff, 1991).

End of the 90's, first transient 3-D snow drift models were introduced, where the wind was determined by computational fluid dynamics. For example, Waechter et al. (1997) compared the velocity field of a flow around an arctic building with observed snow depositions. They estimated that in regions of low velocities snow deposition is possible. Gauer (1999) computed snow transport by saltation based on ballistic grain trajectories. His model included aerodynamic entrainment, ejection of grains due to impacts of other snow particles and particle depositions.

In 2000's substantial suggestions and improvements concerned the combination to snow cover models (Lehning et al., 2008), a simplified deformation of the wind field within the saltation layer (Doorschot and Lehning, 2002) and discussions of the snow drift suspension as a continuum (Liston and Sturm, 1998; Liston et al., 2007; Lehning et al., 2008; Naaim-Bouvet et al., 2010).

Small-scale deposition patterns, such as dunes and cornices, can only be captured by high resolution simulations. Mott and Lehning (2009) investigated the effect of the wind field resolution and obtained the most realistic wind field and deposition patterns down to a resolution of 5 m.

More recently, Schneiderbauer and Prokop (2011) and Mott et al. (2010) were the first, who compared their models with laser scan data. Both models show a linear correlation with laser scan measurements greater than 0.33.

A further challenge of modelling wind flow in complex terrain is the uncertainty connected with boundary and initial conditions. The main concern is how to incorporate remote meteorological data into the definition of the driving wind field. Excepting Schneiderbauer and Prokop (2011), who incorporated data from numerical weather prediction models by a mass conserving optimisation approach after Schneiderbauer and Pirker (2010, 2011), no satisfactory solution has been presented up to now. For instance, extrapolation of weather station data (Gauer, 1999), wind field libraries (Bernhardt et al., 2008) and periodic boundary conditions (Mott and Lehning, 2009) do not provide the necessary flexibility for the operational use in avalanche warning facilities.

Currently, there are several three-dimensional simulation models available, including variable topography, different snow climates and spatially distributed meteorological models. A more detailed review of existing snow drift models is given in Schneiderbauer and Prokop (2011).

To conclude, several main areas are identified which appear most critical for achieving improved results in snow drift simulations (Wurzer, 2010; Schneiderbauer and Prokop, 2011).

1. Application of high-resolution local wind fields, including transient behaviour.
2. Ground surface modelling and the change of surface shape during erosion / deposition events.
3. Assessment of turbulence effects in the air flow.
4. Erosion and deposition behaviour of snow with respect to numerous physical properties like temperature, grain size, wind speed, gross density and erosion rate.

AN ALGEBRAIC SLIP MODEL APPROACH

A fully turbulent non-stationary simulation approach is presented. The main differences to other models are a multiphase Algebraic Slip Model for drifting and blowing snow including time dependent boundary conditions for driving the wind field. These are obtained by a mass conserving optimisation approach applied to meteorological data (Schneiderbauer and Pirker, 2010; 2011).

It is common to distinguish between three different types of snow transport: surface creeping, saltation and suspension (Anderson and Haff, 1991; Bagnold, 1941). Snow transport by surface creeping is commonly neglected in numerical snowdrift models, since its contribution is small compared to the other transport processes.

The snow particles in saltation and suspension are accounted as a continuous phase (Schneiderbauer et al., 2008; Schneiderbauer and Prokop, 2011). This is justified by the physical difference between saltation and suspension as transport modes and lies in the properties of particle trajectories: in saltation, snow particles follow ballistic trajectories as prescribed by their ejection angle and speed; in suspension the motion of the snow grains is affected by the turbulent eddies superimposed by the terminal falling velocity. Snow transport is generally dependent on influencing flow factors, average particle properties (size, shape, etc.) and gravity. The degree of turbulence at the height of the saltation layer is particularly important in determining the number of resuspended snow grains. The ballistic particle trajectories are interrupted by the turbulent velocity fluctuations (i.e. the motion of the turbulent eddies). Therefore no separate numerical domains for the modelling of saltation and suspension are required as in Gauer (1999), Doorschot and Lehning (2002), Liston et al. (2007), Lehning (2008) and Naaim-Bouvet et al. (2010).

Saltation starts if the air borne shear stress, τ, exceeds a certain threshold (Bagnold, 1941) τ_t

$$\tau_t = A^2(\rho_p - \rho_a)gd, \tag{1}$$

where A denotes an empirical parameter, ρ_p the density of the snow particles, ρ_a the density of air, g the standard acceleration due to gravity and d the grain diameter. Erosion of particles by the shear forces exerted by the wind is referred to aerodynamic entrainment. In this work we use a generalized expression for τ_t proposed by Schmidt (1980), which includes the snow bulk properties, microstructure and cohesion

$$\tau_t = 0.056 \frac{(\rho_p - \rho_a) g d (\cos\phi - \sin\phi / \tan\beta + F_C / 4\pi d^2) \tan\theta}{1 + 0.85 \tan\theta}, \tag{2}$$

where $\theta \approx 24°$ denotes the mean drag level, ϕ the slope angle with respect to the flow direction and $\beta \approx 33°$ the angle of repose. It is common to approximate the temperature dependence of cohesion by

$$F_C = 8 F_{C,-15°C} e^{0.141 T}, \tag{3}$$

where T is the temperature. However, there is no general agreement about the value of $F_{C,-15°C}$. The influence of $F_{C,-15°C}$ on snow drift is shown in the parameter study section.

Only a few studies focus on the amount of eroded grains by aerodynamic entrainment. Anderson and Haff (1991) proposed a linear relationship between the entrained grains per unit area, N_{ae}, and the excess air-borne shear stress, $\tau_{\square}$,

$$\frac{\partial N_{ae}}{\partial t} = \xi_{ae} (\tau_E - \tau_t). \tag{4}$$

Anderson and Haff (1991) suggested that the proportionality factor ξ_{ae} does not depend on the wind speed and is approximately 10^5 N^{-1} s^{-1}. This value was also used in many snowdrift models, for example, in Gauer (1999). Shao and Li (1999) found that ξ_{ae} is some magnitudes higher for quartz particle with a diameter of 350 µm, namely, $\xi_{ae} = 5 \times 10^7$ N^{-1} s^{-1}. For smaller particles the value should be even higher.

According to Shao and Li (1999) the initial upward velocity of the entrained snow grains can be approximated by

$$0.5 \sqrt{\tau_a / \rho_a}, \tag{5}$$

where τ_a denotes the air-borne shear stress.

Zones of accumulating snow can be either determined by 'stick-slip' criteria or by using an expression for the rebound probability of snow particles, P_R, proposed by Anderson and Haff (1991). P_R reads

$$P_R(u_i) = 0.95 \left(1 - e^{-u_i / \gamma \sqrt{dg}}\right), \tag{6}$$

where u_i is the impact velocity of impacting snow particles and $u_i / \gamma \sqrt{gd}$ defines a velocity scale with $\gamma \approx 10$. The number of accumulating snow grains, N_a, can therefore be written as

$$\frac{\partial N_a}{\partial t} = \frac{\partial N_i}{\partial t} (1 - P_R(u_i)). \tag{7}$$

In equation (7) $\partial N_i / \partial t$ denotes the number of impacting grains per unit time and unit area. To obtain an expression for the impact velocity of the saltating snow grains we follow Pomeroy and Gray (1990), who suggested that the horizontal particle velocity within the saltation layer is constant with height. We also assume that the flow velocity matches the particle velocity at the top of the saltation layer with height h_s implying

$$u_i = u_{h_s} = u_a(h_s). \tag{8}$$

Typically h_s is O(<10^{-1}) m (Anderson et al., 1991) and can be derived from (Greeley and Iversen, 1985)

$$h_s = 1.6 \frac{\tau_a}{\rho_a g}. \tag{9}$$

Since we model the snow transport by a passive transport equation, which neglects the interphase momentum exchange, the wind field is not influenced by the snow grains in terms of the force required to accelerate rebounded, entrained and ejected particles. Hence, the excess airborne shear stress, $\tau_{\square}$, appearing in Equation (4) – the shear stress available for aerodynamic entrainment – remains unknown. Thus, we compute $\tau_{\square}$ from a local momentum balance at the snow cover:

$$\tau_E = \tau_a - \tau_R - \tau_\phi, \tag{10}$$

where τ_R denotes the shear stress appearing from particle rebounds and $\tau_{\square}$ the shear stress from a non-zero slope. Particle ejections are neglected in this work. The air-borne shear stress τ_a can be determined directly from the wind field. The parameterizations of τ_R and $\tau_{\square}$ can be found in Schneiderbauer and Prokop (2011).

Finally, the topology is modelled dynamically to account for the surface change by deposition and erosion.

ADVANCED SIMULATION OF SNOW DRIFT

Numerical grid

For the numerical analysis of wind flow and snow transport at the Planneralm site a hexahedral finite volume mesh is used. The horizontal extensions of the analysis domain are 7.8 km in west-east and north-south direction, which is slightly smaller than the ALADIN-Austria Weather Prediction Model grid resolution of 9.6 km. The top boundary is located 2.5 km above the Gstemmer peak. The horizontal resolution of the finite volume grid is 10 m around the wind reference station on top of the Gstemmer peak, which is linearly expanded towards the boundaries of the analysis domain. The heights of the vertices at the surface level are bilinearly interpolated from a 25 m resolved digital elevation model (DEM) dataset.

Influence of different snow properties and of the driving wind field to snow drift

The dependency of the computed snow depth to various snow properties, i.e. wind speed u_a, ξ_{ae}, F_c, ρ_p and d, is analysed. The flow field at t = 4 h at the 3rd Feb. 2010 (see next section, figures 5a,b) is used to drive snow drift. The final snow depth is evaluated at t = 5 h.

In figures 2a and 2b the difference of the snow depth $dh_S \left(= h_S(t=5) - h_S(t=4)\right)$ is plotted for different values of ξ_{ae} and F_c (equations (3) and (4)). Corresponding plots for the variations of dh_S for different values of d and ρ_p are shown in figures 3a and 3b. Note that at the snow reference station snow is eroded and at the snow poles snow is deposited (compare with figure 7). From the figures one can deduce:

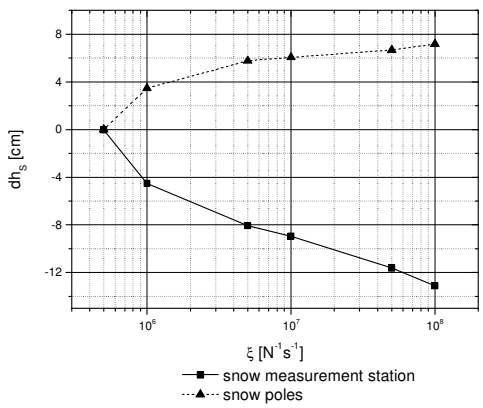

(a) dh_S for different values of ξ_{ae} (F_C = 0 N)

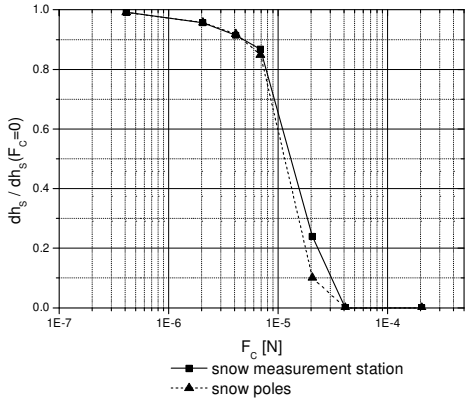

(b) $dh_S/dh_S(F_C = 0)$ for different values of F_C ($\xi_{ae} = 10^6$ N^{-1}s^{-1})

Fig. 2 Variation of dh_S for different values of ξ_{ae} and F_C (ρ_p = 500 kg m^{-3}, d = 500 µm)

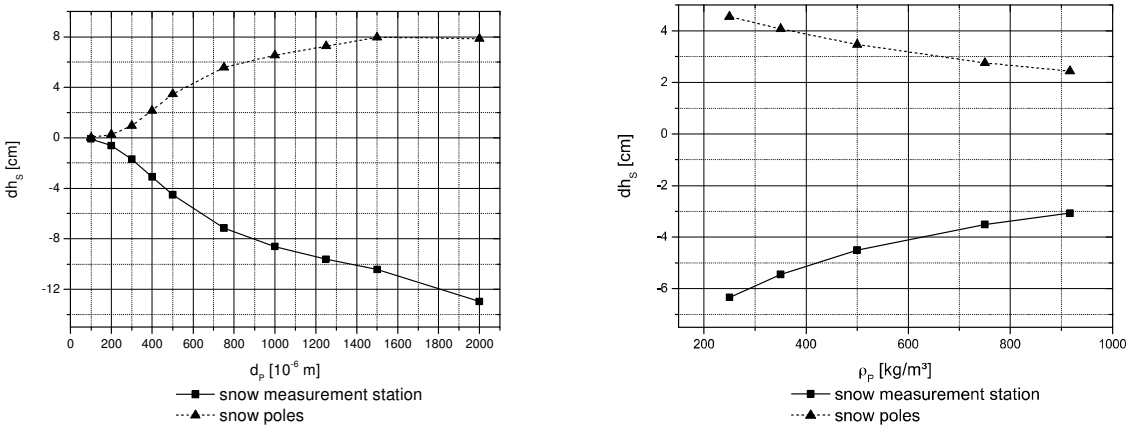

(a) dh_S for different values of d (ρ_p = 500 kg m^{-3}) (b) dh_S for different values of ρ_p (d = 500 µm)

Fig. 3 Variation of dh_S for different values of ρ_p and d (ξ_{ae} = 10^6 N^{-1} s^{-1}, F_C = 0 N)

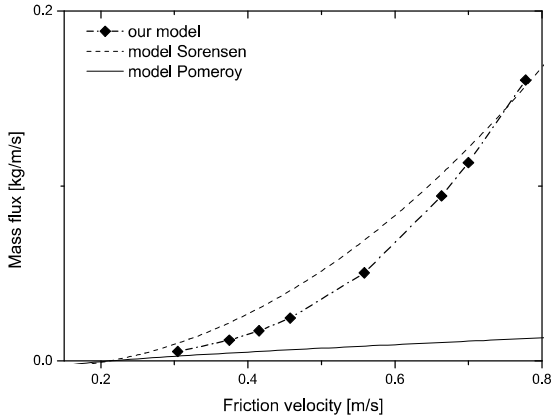

Fig. 4 Dependence of the saltation mass flux on the friction velocity, u_*. -◆- our model (Wurzer, 2010), – Pomeroy and Gray (1990), --- Sorensen (1991); ρ_p = 500 kg m^{-3}, d = 500 µm, ξ_{ae} = 5x10^6 N^{-1} s^{-1}, F_C = 0 N.

1. The amount of erosion with respect to the air borne shear stress: Using a parameter magnitude as suggested in literature (ξ_{ae} = 10^5 N^{-1} s^{-1}) leads to significantly less drift at Planneralm compared to measurements (figure 2a). Increasing the parameter by one order of magnitude delivers good correlation of measurement and simulation (compare with figure 6a). Increasing the parameter by factor 100, results in change of snow height by approx. factor 2 to 3. Hence, in a wide parameter range snow drift is relatively insensitive to an error in the estimation of ξ_{ae}.
2. For low cohesion the amount of redistributed snow changes just about 15%, when increasing the cohesive force approximately by a factor 10 (figure 2b). Snow drift, however, stops, if the cohesive force per unit area exceeds the air borne shear stress.
3. Grain diameter: The amount of eroded snow at the snow measurement station depends linearly on the grain diameter (figure 3a). For approximately 1.5 to 2mm grains, snow drift approaches a maximum level of sedimentation at the snow poles (figure 3a). Note that the grain diameter hardly depends on temperature and varies from 50 µm for rather rounded particles at low temperatures to more than 1 mm for dendrites around 0°C.
4. Particle density: Varying the density between 200 and 900 kg m^{-3}, the amount of redistributed snow changes less than 50% (figure 3b). This holds for accumulation as well as for erosion zones.
5. Saltation mass flux: A modification of the friction velocity by the factor two leads to a change of the snow particle flux rate by the factor 8 (figure 4). Hence, the model is able to reproduce

the saltation mass flux to the expected scale of u_*^3 (Clifton and Lehning, 2008) in contrast to the relation proposed by Pomeroy and Gray (1990)

$$q = 0.68 \frac{\rho_a u_{*t}}{g u_*} \left(u_*^2 - u_{*t}^2 \right). \tag{11}$$

The relation given by Sorensen (1991)

$$q = 0.0014 \rho_a u_* \left(u_* - u_{*t} \right) \left(u_* + 7.6 u_{*t} + 205 \right) \tag{12}$$

also predicts that the saltation mass flux to the expected scale of u_*^3. u_* denotes the friction velocity $u_* = \sqrt{\tau_a / \rho_a}$.

Therefore, the driving wind field is identified as the most sensitive modelling parameter.

Analysis of time dependent boundary conditions and validation of snow drift model

In the last section we found that an accurate determination of the driving wind field is inevitable when simulating environmental snow transport. Hence, additionally to the determination of the snow properties the questions of

- an appropriate definition of the spatial boundary conditions for the driving environmental fluid flow
- and the atmospheric turbulence effecting the dispersion of the snow grains in suspension

arise.

The first question is addressed by utilizing a mass conserving optimization approach to determine the open boundary conditions from punctual observations within the analysis domain (Schneiderbauer and Pirker, 2010). The Numerical Weather Prediction (NWP) model ALADIN–Austria provides wind speed and wind direction at those spatially arbitrarily defined observations.

The second question is addressed by using the RNG k–ε model, which meets the demands of turbulence modelling in mountainous regions. At the lateral boundaries, analytical vertical turbulence profiles ensure appropriate turbulent intensities in the atmospheric boundary layer (e.g. Wurzer 2010).

The flow over the Planneralm is computed time dependent, where the commercial flow solver FLUENT is used to solve the flow equations. The analysis of the unsteady wind field at the Planneralm is based on an hourly ALADIN-Austria forecast. The role of the temporal resolution of the weather data is discussed in Schneiderbauer and Pirker (2010, 2011). For two years, measurements and analysis of snow drift were successfully compared for the Planneralm test site. Two significant wind scenarios, where considerable redistribution of snow occurred, are presented in the following:

- 3rd of February 2010 starting at 0600 CET (Central European Time); snow drift event between 1000 CET and 1100 CET
- 18th of March 2011 starting at 0700 CET, snow drift for 6 hours.

In figure 5 comparisons of the model results and the measured wind speed and wind direction at the wind reference station, which is on top of the Gstemmer peak, and at the snow station are shown (figure 1).

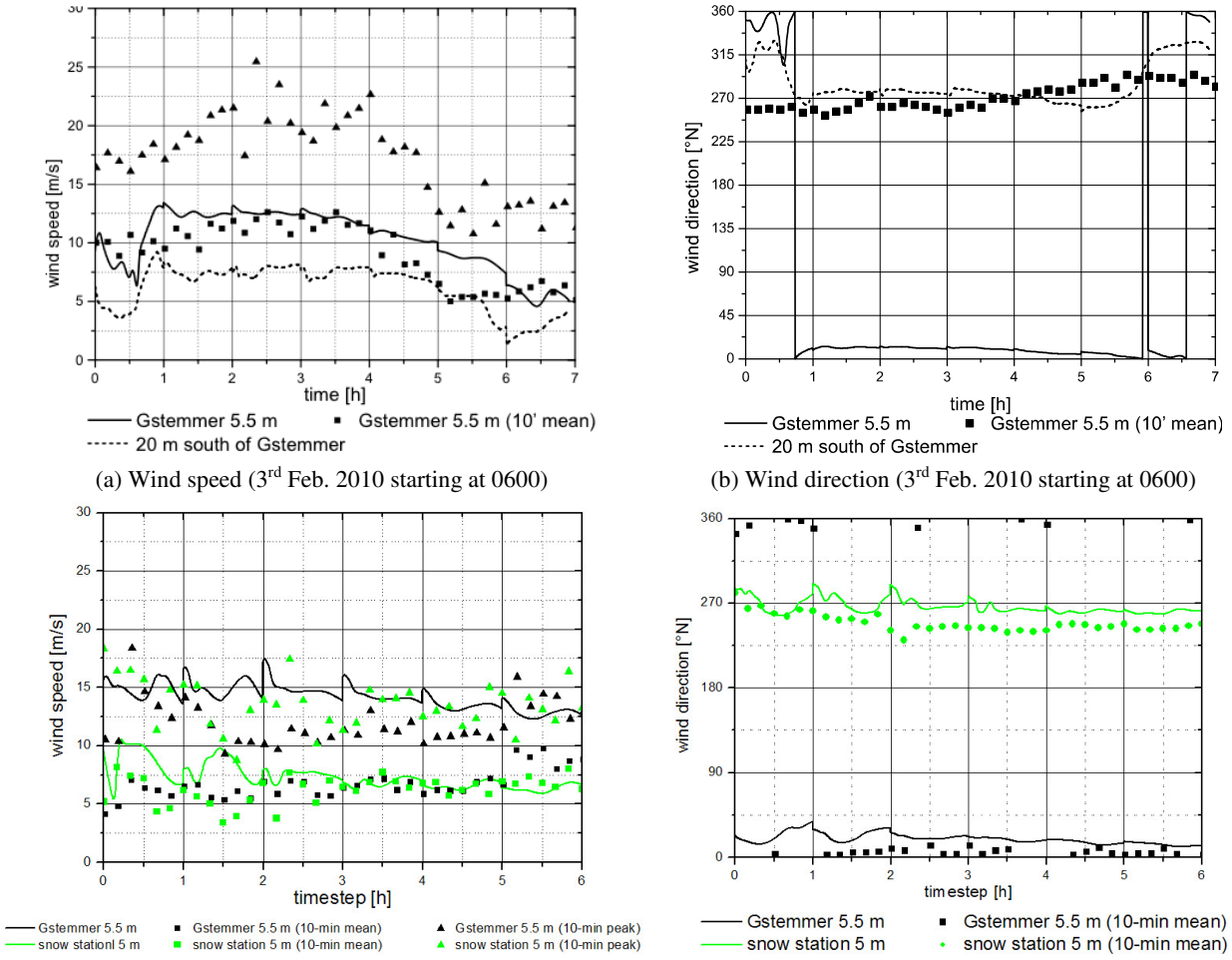

(a) Wind speed (3rd Feb. 2010 starting at 0600)

(b) Wind direction (3rd Feb. 2010 starting at 0600)

(c) Wind speed (18th March 2011 starting at 0700)

(d) Wind direction (18th March 2011 starting at 0700)

Fig. 5 Comparison of measured (symbols) and computed (lines) wind speeds and directions at the Gstemmer peak (black) and at the snow station (green); a,c) Wind speeds: The **squares** correspond to the measured 10 min averaged wind speeds and the **triangles** to wind peaks within these 10 min intervals; b,d) Wind directions: The **circles** and **squares** correspond the measured 10 min averaged wind directions at the snow reference station and the Gstemmer peak, respectively.

After t = 1 h at the 3rd Feb. 2010 the wind speed is in satisfactorily agreement with the measured values at the Gstemmer peak (figure 5a). In contrast, for this scenario figure 5b shows that the wind direction at the reference station differs from the measurements considerably. This deviation is probably due to the coarse resolution of 25 m of the underlying DEM data (refer to previous subsection), which causes a smoothening of the Gstemmer peak in the numerical grid compared to reality. Evaluating the computed wind direction 20 m southward of the Gstemmer reference station shows a good agreement with measurements (dotted line in figure 5b). At global westerly winds the flow is canalized through the valley located on the north side of the Gstemmer peak, which leads to a conjunction of local westerly and northerly wind. This effect is shown in figure 7.

At the 18th March 2011 the wind speed is slightly overestimated at the Gstemmer reference station by the numerical model (figure 5c). More important, at the snow station the computed wind speed well predicts the measurements, which is inevitable to accurately compute the amount of redistributed snow (figure 5c). At both locations the wind direction corresponds well to the measurements (figure 5d).

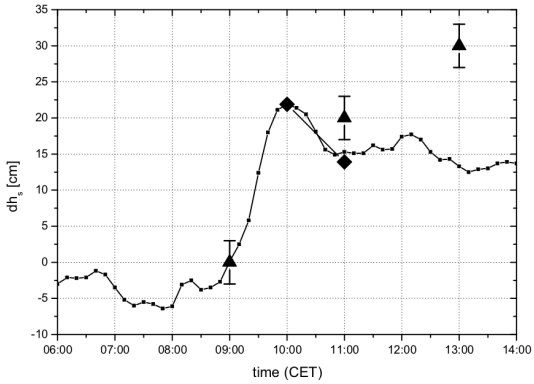

(a) 3rd Feb. 2010; **aligned squares**: measured dh_S at snow reference station; ◆ simulated dh_S at snow reference station; **triangles**: measured dh_S at snow poles.

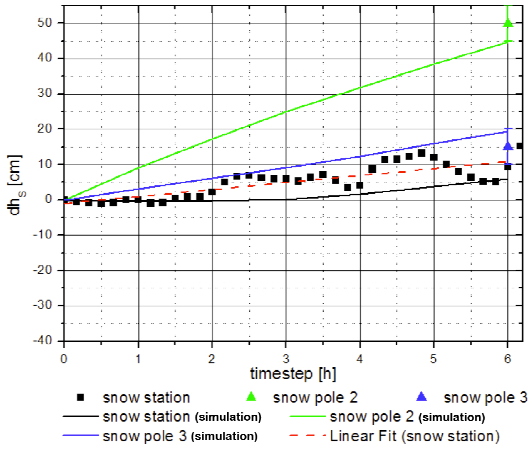

(b) 18th March 2011; **solid lines**: simulated dh_S; **squares**: measured dh_S at snow reference station; **triangles**: measured dh_S at snow poles; **dashed line**: linear fit of the measured dh_S at the snow reference station.

Fig. 6 Variation in time of dh_S at the snow reference station and the snow poles ($\xi_{ae} = 5\text{x}10^6$ N^{-1} s^{-1}, $F_C = 0$ N, $d = 500$ µm, $\rho_p = 500$ kg m^{-3}). The error bars indicate the uncertainty of the image interpretation of the webcam snow pole images.

To validate the presented model, the results for the drift events at the 3rd Feb. 2010 and 18th March of 2011 are compared to the measured snow depth at the snow reference station and at snow poles (figures 1 and 6). The bulk density of the snow cover, ρ_b, is assumed as a dense packing of snow grains with $\rho_p = 500$ kg m^{-3} yielding $\rho_b \approx 0.6\rho_p$. The snow reference station is located on a small ridge in downhill direction, which is touched by a chute on the east side. The automatic Ultrasonic snow depth sensor USH-8 with a resolution of 1 mm and an accuracy of 0.1 % (FS) measures the snow depth every 10 seconds and returns the 10 minute

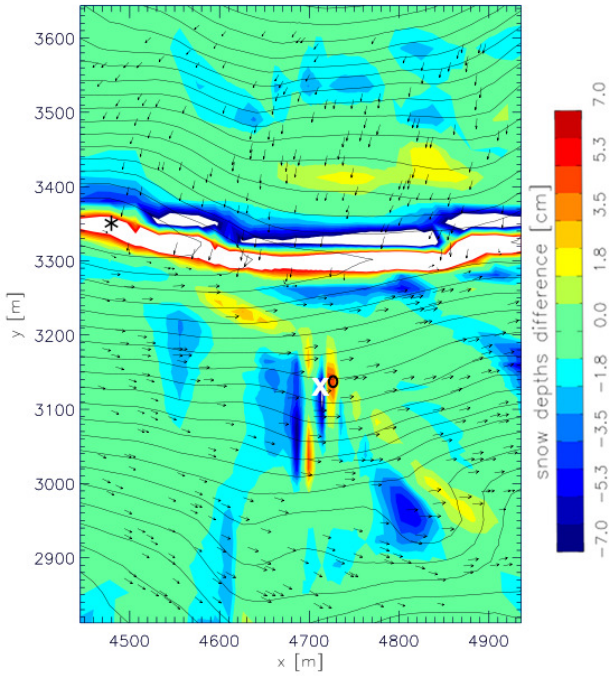

Fig. 7 Redistribution of snow by blowing and drifting snow ($\xi_{ae} = 5\text{x}10^6$ N^{-1} s^{-1}, $F_C = 0$ N, $d = 500$ µm, $\rho_p = 500$ kg m^{-3}) from 1000 CET to 1100 CET, 3rd Feb. 2010. The vectors represent the wind 5 m above the surface. **X** indicates the position of the snow reference station and **O** the position of the snow poles. * indicates the weather station at the Gstemmer peak. The contour lines represent a distance interval in z-direction of 15 m.

average. The snow depth at the snow poles is taken from webcam pictures with an accuracy of ± 3 cm.

Until 1000 CET (t=4 h) at Feb. 3 2010 the snow depth at the station increased due to precipitation. Afterwards the snow depth decreased at the station because of erosion by high wind speeds during approximately 1 hour (figure 6a). The observed decrease of 7 cm is in good agreement with the computed change in snow depth, dh_S, which was 8 cm in 1 hour (figure 6a). In this case cohesion was neglected because of the low air temperature of -7°C and fresh powder snow (Schmidt, 1980). The increase of snow depth at the snow poles can only be compared qualitatively since the snow heights were measured in 2 hours intervals. However, the simulation predicts an amount of accumulated snow of approximately 10 cm, which well corresponds with the webcam images of the snow poles.

In figure 6b the change in snow depth, dh_S, at the snow reference station and at the snow poles at the 18th March 2011 is plotted. Due to the high negative temperatures cohesion is also neglected during this event. In contrast to the snow drift event at the 3rd Feb. 2010, precipitation with a rate of 4 cm h^{-1} occurs during this drifting period. The precipitation rate was measured at the Planneralm station. The freshly fallen snow overcompensates snow erosion at the reference station, which leads to an effective increase of the snow height. At the snow poles, where accumulation of drifting snow prevails, the deposition rate is therefore increased. The simulation results are in good agreement with the measurements at the snow reference station and the snow poles.

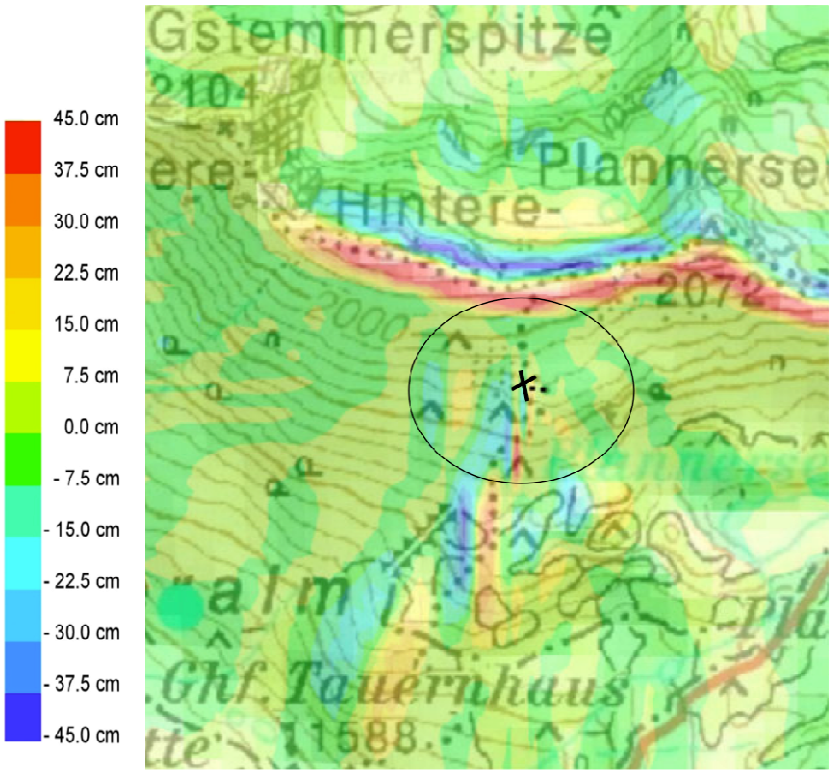

Fig. 8 Redistribution of snow by drifting snow and precipitation from 0700 CET to 1300 CET, 18th March 2011 (ξ_{ae} = 5x10^6 N^{-1} s^{-1}, F_C = 0 N, d = 500 µm, ρ_p = 500 kg m^{-3}). **X** indicates the position of the snow reference station and • the position of the snow poles.

Additional to the punctual comparison of figure 6, the computed area-wide redistributions of snow are shown in figures 7 and 8. The results are in good agreement with experts experiences for this area. The simulation shows accumulation of snow in leeward slopes, chutes and dingles. Erosion of snow occurs at the ridges. Also, a typical and well known snow cornice at the Gstemmer peak is correctly reproduced by the simulation.

CONCLUSIONS

The parameter study shows the influence of important snow property parameters to the simulated snow height. However, the snow drift simulation is much more sensible to the variation of wind conditions than to the variation of snow properties in typical ranges. An accurate assessment of the local wind field and its turbulence effects is inevitable for predicting snow drift.

The determination of time dependent boundary conditions from macro- and meso-scale Numerical Weather Prediction (NWP) models by optimization techniques is a good base for micro-scale alpine wind field computations and for snow drift simulations. The results of the snow drift simulation fit the measured data satisfactorily. The snow drift simulation provides information about the local snow depth in the whole analysis domain. It can provide an important support for avalanche warning and decisions of avalanche commissions (Studeregger et al., 2012). It remains of vital importance to consider online weather data for the prediction of snow depositions for operational avalanche warning.

Nevertheless, it is acknowledged that snow parameters have an important role and additional work has to be done on the important effect of the metamorphosis of snow.

REFERENCES

Anderson R.S., Haff P.K. (1991). Wind modification and bed response during saltation of sand in air. Acta Mechanica, 1, 21–51.

Anderson R.S., Sorensen M., Willets B.B. (1991). A review of recent progress in our understanding of aeolian sediment transport. Acta Mechanica 1. 1–19

Bagnold R. (1941). The physics of blown sand and desert dunes. Methuen and Co, London.

Bernhardt M., Zängl G., Liston G.E., Strasser U., Mauser W. (2009). Using wind fields from a high resolution atmospheric model for simulating snow dynamics in mountainous terrain. Hydrol. Process., 23(7), 1064–1075.

Doorschot J., Lehning M. (2002). Equilibrium Saltation: Mass Fluxes, Aerodynamic Entrainment and Dependence on Grain Properties. Boundary-Layer Meteorology, 104(1):111–130.

Clifton A., Lehning M. (2008). Improvement and validation of a snow saltation model using wind tunnel measurements. Earth Surf. Process. Landf., 33(14), 2156–2173.

Fell R., Ho K.K.S., Lacasse S., Leroi E. (2005). A framework for landslide risk assessment and management. In Hungr, O., R. Fell, R. Couture and E. Eberhardt, eds. Landslide risk management. London, Taylor and Francis.

Gauer P. (1999). Blowing and Drifting Snow in Alpine Terrain: A Physically Based Numerical Model and Related Field Measurements. PhD Thesis, SLF Davos.

Greeley R., Iversen J.D. (1985). Wind as a geological process on Earth, Mars, Venus and Titan.
Cambridge, Cambridge University Press.

Lehning M., Löwe H., Ryser M., Raderschall N. (2008). Inhomogeneous precipitation distribution and snow transport in steep terrain. Water Resour. Res., 44(W7).

Liston G. E., Sturm M. (1998). A snow-transport model for complex terrain. Journal of Glaciology, 44(148):498–516.

Liston G.E., Haehnel R.B., Sturm M., Hiemstra C.A., Berezovskaya S., Tabler R.D. (2007). Simulating complex snow distributions in windy environments using SnowTran-3D. J. Glaciol., 53(181), 241–256.

Mott R., Lehning M. (2009). Meteorological Modelling of Very High-Resolution Wind Fields and Snow Deposition for Mountains. Journal of Hydrometeorology, 11:934–949.

Mott R., Schirmer M., Bavay M., Grünewald T., Lehning M. (2010). Understanding snow-transport processes shaping the mountain snow-cover. Cryosphere, 4(4), 545–559.

Naaim-Bouvet F., Bellot H., Naaim M. (2010). Back analysis of drifting-snow measurements over an instrumented mountainous site. Ann. Glaciol., 51(54), 207–217.

Pomeroy J., Gray D. (1990). Saltation of snow. Water Resour. Res., 26(7):1583–1594.

Schmidt R. (1980). Threshold wind-speed and elastic impact in snow transport. Journal of Glaciology, 26(94):453–467.
Schneiderbauer S., Pirker S. (2010). Resolving Unsteady Micro Scale Atmospheric Flows by Nesting a CFD Simulation into Wide Range Numerical Weather Prediction Models. International Journal of Computational Fluid Dynamics, 24(1):51–68.
Schneiderbauer S., Pirker S. (2011). Determination of Open Boundary Conditions for Computational Fluid Dynamics (CFD) from Interior Observations. Applied Mathematical Modelling, 35(2):763–780.
Schneiderbauer S., Prokop A. (2011). The atmospheric snow-transport model: SnowDrift3D. Journal of Glaciology, 57(203):526–542
Schneiderbauer S., Tschachler T., Fischbacher J., Hinterberger W., Fischer P. (2008). Computational fluid dynamic (CFD) simulation of snowdrift in alpine environments including a local weather model for operational avalanche warning. Annals of Glaciology, 48:150–158.
Shao Y., Li A. (1999). Numerical Modelling of Saltation in the Atmospheric Surface Layer. Boundary Layer Meteorology, 91:199–225.
Sorensen M. (1991). An analytic model of Wind-Blown sand transport. Acta Mechanica (Supplementum), 1:67–81.
Studeregger A., Rieder H., Ertl W., Zenke B. (2012). Interprätation von Daten von meteorologischen Stationen als praktische Grundlage für die Entscheidungsfindung für Lawinenkommissionsmitglieder und für Lawinenwarndienste. Interpraevent 2012, Grenoble, France.
Waechter B. F., Sinclair R. J., Schuyler G. D., Williams C. J. (1997). Snowdrift Control Design: Applicaton of CFD Simulation Techniques. Proceedings of the Third International Conference on Snow Engineering, Sendai, Japan. 511–516.
Wurzer A. (2010). Validation of a Snow Drift Model at the Planneralm, Austria. Masters Thesis, Karl-Franzens-Universität Graz, Austria.
Wurzer A., Studeregger A., Fischer P. (2010). Critical Review of challenges and potentials for snow drift simulation. Proceedings of the International Snow Science Workshop 2010, Squaw Valley, CA, USA.